Surface-enhanced Raman scattering from ordered Ag nanocluster arrays

Jason P. Schmidt, Sarah E. Cross, and Steven K. Buratto
Department of Chemistry and Biochemistry, University of California, Santa Barbara, California 93106

(Received 26 June 2003; accepted 5 August 2004)

We have examined the effect of ordered silver nanocluster substrates on the surface-enhanced Raman spectrum of rhodamine 6G (R6G). Triangular shaped silver nanocluster arrays with order on the ~100 μm range were prepared using nanosphere lithography. Direct comparisons of R6G surface-enhanced Raman spectroscopy (SERS) signals between ordered nanocluster regions and amorphous Ag regions prepared under identical deposition conditions provide strong evidence of an electromagnetic field enhancement attributed to the unique nanocluster morphology. We have obtained order of magnitude enhancement factors for both 200 and 90 nm Ag nanocluster SERS substrates relative to Ag films. © *2004 American Institute of Physics.* [DOI: 10.1063/1.1799992]

I. INTRODUCTION

Metallic nanoclusters have received considerable attention due to their potential in optical sensing,[1,2] optoelectronics,[3,4] and catalysis.[5,6] Metal-based nanomaterials have also found application in the field of surface-enhanced Raman spectroscopy (SERS).[7,8] For over 20 years it has been known that a rough metal surface of Ag or Au can enhance the electric field in resonance with surface plasmons by several orders of magnitude. This field enhancement has led to the detection of Raman scattering from molecules adsorbed to the metal films with sensitivity approaching that of molecular fluorescence. Theory predicts that the field enhancement can become extremely large in the region near a sharp metallic point or in the region between two small metal spheres which are often referred to as ''hot spots'' in the film.[9–12] Recent experiments have demonstrated that these hot spots can lead to extremely sensitive Raman spectroscopy with a detection limit of a single molecule.[13–15]

While numerous groups have successfully detected increased SERS signals by modifying the deposition parameters of metal films in order to increase the concentration of hot spots, there have been few efforts in fabricating SERS substrates using lithography.[16–18] It would be advantageous to exploit the large fields such as those generated by sharp, fractallike structures, if these features could be prepared in a controlled, reproducible manner over large areas.[19,20]

In this report we have used the simple, yet elegant technique of nanosphere lithography pioneered by Van Duyne and co-workers to generate large arrays of ordered, sharp triangular Ag nanoclusters in order to enhance electric fields at the nanocluster vertices.[21–23] These metal nanostructures were then used as the SERS substrate and the Raman spectra of rhodamine 6G molecules adsorbed to these nanoclusters were acquired. The SERS enhancement for the nanoclusters was then compared directly with the enhancement from neighboring amorphous Ag regions with identical surface roughness. On average, we show that the SERS signal increases by an order of magnitude relative to that of the Ag films when the spectra are taken in the triangular nanocluster regions.

II. EXPERIMENT

White latex (polystyrene) nanospheres (900 and 400 nm) with negatively charged carboxylate ligands and ≈4 wt % (in H_2O) were obtained from Interfacial Dynamics Corp. and used without further purification. For deposition of both the 900 and 400 nm spheres, stock solutions were diluted to roughly 2 wt %. A 2 μl aliquot was drop cast onto a treated glass surface. Prior to deposition, glass substrates (Fisher no. 2) were immersed in Piranha (3:1; H_2SO_4:H_2O_2) for 15–20 min, rinsed with H_2O, sonicated in RCA (5:1:1; H_2O:NH_4OH:H_2O_2) for 40 min, and then rinsed again with H_2O. The substrate is dried with N_2 between steps. Bullen and Garrett have shown that the area of the ordered monolayer regions often increases with angle deposition.[24] We have achieved the largest areas of order (~300×300 μm^2) by drop casting the colloidal droplet onto a substrate held at a 10° angle. The area of ordered monolayer regions of nanospheres is monitored using reflectance microscopy and atomic force microscopy (AFM).

After successful formation of monolayer regions samples are inverted and placed in a vacuum deposition chamber. Silver deposition is performed normal to the surface at 10^{-5}–10^{-6} torr with a resistively heated tungsten filament. From earlier SERS experiments done on Ag films, we determined that suitably rough films resulted from evaporation at a rate of ~1 Å/s. Film thicknesses vary with the particular application, but the experiments herein were performed on ~10 nm films. In each sample, a portion of the slide was kept clear of nanospheres in order to produce a region of pure Ag film. After metal evaporation, the nanospheres were removed by sonication in 100% ethanol for 3 min.

Nanocluster arrays were imaged using Digital Instruments D3000 and D3001 atomic force microscopes in tapping mode. Ordered regions were first located using the white light camera mounted on the scanning stage. Samples were typically imaged at a scan rate of 0.5 Hz with 256×256 lines/image. The root-mean-squared (rms) roughness, defined as the variation in the height of the silver grains of each nanotriangle, was determined from the AFM image for a

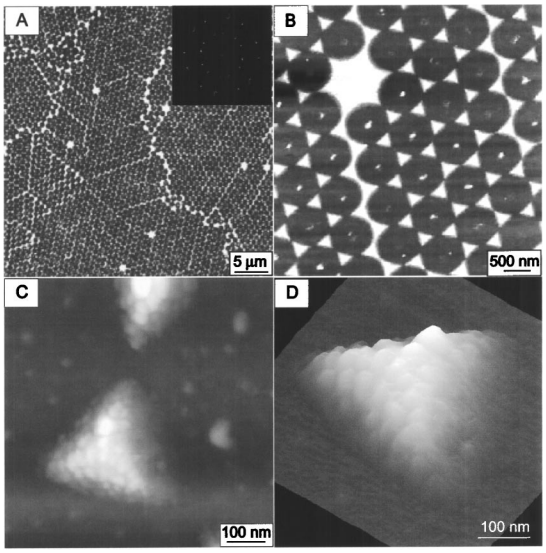

FIG. 1. AFM images of ~200 nm clusters made from 900 nm polystyrene spheres. Image (a) is a 40×40 μm^2 with the 2D FT shown in the inset. A 5×5 μm^2 image illustrating a single nanosphere vacancy is shown in (b), and a 500×500 nm^2 image of a single pair of nanoclusters is shown in (c). A 3D rendering of a single cluster demonstrating the faceted surface is shown in (d).

statistical sample (>100) of nanoclusters and compared to the rms roughness of a silver film. This provides a direct comparison of the silver grain size within a silver nanoparticle with the grain size within a silver film.

All SERS measurements were performed with an upright confocal microscope. The 488 nm line of an argon ion laser was attenuated to ~600 μW (Spectra Physics 2010), sent to a 1.25 NA oil immersion objective (Zeiss) and focused to a spot size of ≈300 nm. SERS spectra were obtained using a 0.27 m spectrometer with a 1200 line/mm grating and a liquid N_2 cooled charge-coupled device (Princeton). Independent experiments of SERS on 60–100 Å Ag films in our group show that electromagnetic hot spots are completely saturated above 250 μM R6G concentration. To alleviate dye heterogeneity/adsorption issues, samples were made by drop casting 1 μl of a 1 mM R6G aliquot to saturate the entire metallic region, which includes the areas of pure Ag film.

III. RESULTS AND CONCLUSIONS

Topography images of ordered Ag nanostructure arrays prepared by nanosphere lithography are shown in Fig. 1. The triangular clusters shown in Figs. 1(a)–1(d) were prepared from a mask of 900 nm spheres, which results in a cluster size of ~200 nm. The image shown in Fig. 1(a) is from a 40×40 μm^2 scan, close to the scan size limit permitted by the AFM scanning head. The inset of Fig. 1(a) shows a two-dimensional (2D) Fourier transform of the 40×40 μm^2 image and indicates the degree of order achieved. A number of interesting features are evident in the image of Fig. 1(a). First, all bright regions indicate the presence of metal. The majority of the bright features shown in the 40×40 μm^2 image are the triangular Ag nanoclusters expected from the nanosphere mask.[21] In addition to these triangular features, characteristic defects are also observed. Continuous jagged, asymmetric dislocations separate ordered nanocluster regions on a 10–50 μm scale. Linear, misfit dislocations also separate approximately every 5–10 rows of nanoclusters. These defects result from nanospheres that are not completely close packed. As a result, the metal is able to penetrate between adjacent spheres and produce a continuous line of metal. These features represent only a few percent of the surface and are observed for all nanosphere masks. Single nanosphere vacancies are also observed in Figs. 1(a) and 1(b) and are characterized by the small, white star shapes in the image.

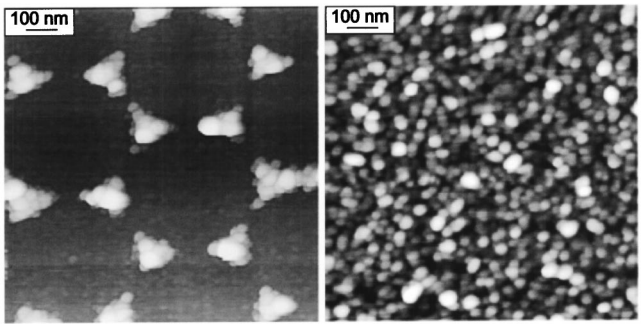

FIG. 2. 1×1 μm^2 AFM images of a 90 nm nanocluster region and a neighboring "amorphous" Ag region where SERS comparisons were taken from showing the identical surface roughness.

Figure 1(b) shows a 5×5 μm^2 image displaying the crisp, well-resolved edges of the hexagonally packed triangles and also shows a single star-shaped nanosphere vacancy. The bright spots in the center of each circular void region are due to residual metal that falls off the nanospheres during the sonication process and then sticks to hydrophobic regions containing nanosphere residue. These can be removed from the substrate using nonpolar solvents. Figure 1(c) is a 500×500 nm^2 image of a single pair of triangular nanoclusters. The individual nanoclusters are characterized by sharp triangular edges and have a rough internal structure identical to the amorphous Ag film (see Fig. 2). The distance of closest approach between neighboring nanoclusters prepared from 900 nm spheres is between 50 and 70 nm. At this distance, theory predicts negligible coupling between adjacent nanoclusters.[9] Figure 1(d) shows a 3D rendering of a single nanocluster from Fig. 1(c). The surface is faceted and resembles a truncated tetrahedron as expected.[25]

Surface-enhanced Raman experiments performed on nanocluster arrays such as those shown in Fig. 1 have two potential electric field enhancement mechanisms: (i) enhancement due to the surface roughness analogous to an Ag film and (ii) enhancement due to the nanocluster size and shape (particularly the sharp points of the triangles). In order to separate these enhancement effects, both triangular Ag clusters and amorphous Ag film regions were produced on the same substrate. A comparison of these two regions is presented in Fig. 2. In Fig. 2, 1×1 μm^2 AFM images were taken of triangular 90 nm clusters produced from a mask of 400 nm spheres [Fig. 2(a)], and a neighboring amorphous Ag film region [Fig. 2(b)]. The rms roughness within the nanoclusters and in the Ag film are identical and equal to ≈5 nm rms. For all of our nanoparticle and amorphous film samples

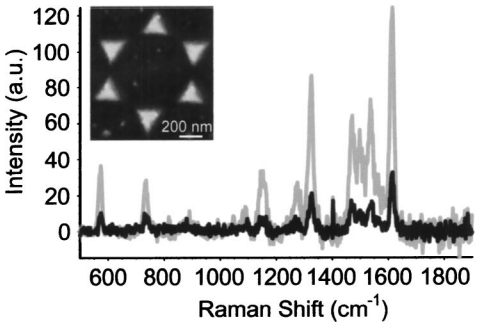

FIG. 3. SERS enhancement achieved from R6G adsorbed on ordered 200 nm Ag nanocluster regions (gray trace) in comparison with amorphous Ag "film" regions (black trace) within the same sample. The signal increase is ~3×.

fabricated simultaneously we observed identical rms roughness for the nanoclusters and the silver film. Thus, SERS signals obtained from molecules adsorbed to each region will provide a relative comparison of the two enhancement effects. Any additional field enhancement observed for the Ag nanoclusters in comparison with the Ag film must come from the shape of the cluster rather than the roughness.

Figures 3 and 4 show the SERS enhancement associated with morphology for both 200 and 90 nm nanoclusters. For both Figs. 3 and 4, the black, bottom trace was taken in a large, amorphous silver region. The gray, top trace was acquired by focusing on an ordered nanocluster region. The spectra shown were background substracted to remove residual dye fluorescence and in order to directly compare the two signals. Figure 3 illustrates the SERS enhancements for R6G adsorbed to 200 nm triangular nanoclusters. An increase of a factor of 3 was achieved. A factor of 2.6 was achieved for R6G adsorbed to the 90 nm Ag nanoclusters as shown in Fig. 4. Due to control experiments and roughness comparisons performed with Ag film regions, we attribute the enhancements for each case to edges and corners of the triangular nanoclusters. It is also important to note that the Raman signal from the Ag film (gray line) represents the maximum observed. The signal over the Ag film was found to vary in position by an order of magnitude. The signal from the Ag nanoclusters (black lines) did not vary by more than a few percent from one nanocluster to the next.

In order to compare the SERS signals obtained from the nanocluster and film region more quantitatively it is important to note that the amount of Ag within the beam spot is different for each case. Assuming a beam waist of 300 nm, only one nanocluster is in the field of view on average for the 200 nm clusters, which amounts to ~33% of the metal illuminated in the Ag film. Accounting for this difference the true enhancement factor of the Ag nanoclusters over the Ag film is a factor of 9, rather than 3 as determined from the data in Fig. 3. A similar calculation for the 90 nm clusters results in an average of three nanoclusters in one beam spot and a true enhancement factor of roughly 13.

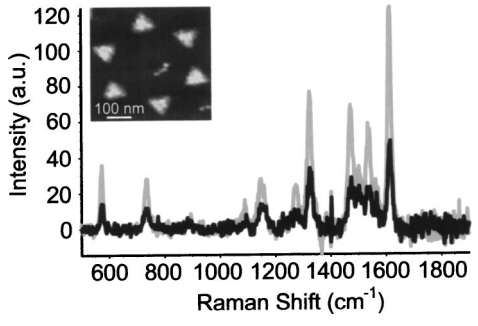

FIG. 4. SERS enhancement for 90 nm clusters (gray trace) in comparison with the Ag film region (black trace) within the same sample. Enhancements are roughly a factor of 3.

In summary, we have shown that SERS of R6G on ordered 200 and 90 nm Ag nanoclusters prepared by nanosphere lithography show an order-of-magnitude enhancement relative to amorphous Ag films (measured to be of the order of 10^6 in our experiments). The direct comparisons of SERS intensities with neighboring amorphous Ag regions provide strong evidence for large local electromagnetic fields at the corners of the triangular nanoclusters. High spatial resolution near-field Raman experiments are currently underway to map the electromagnetic fields generated from individual nanoclusters.

ACKNOWLEDGMENT

The authors wish to gratefully acknowledge AFOSR/DURINT for funding this work.

[1] K. E. Shafer-Peltier, C. L. Haynes, M. R. Glucksberg, and R. P. Van Duyne, J. Am. Chem. Soc. **125**, 568 (2003).
[2] A. J. Haes and R. P. Van Duyne, J. Am. Chem. Soc. **124**, 10596 (2002).
[3] T.-H. Lee and R. M. Dickson, Proc. Natl. Acad. Sci. U.S.A. **100**, 3043 (2003).
[4] C. D. Keating and M. J. Natan, Adv. Mater. (Weinheim, Ger.) **15**, 451 (2003).
[5] M. X. Yang, D. H. Gracias, P. W. Jacobs, and G. A. Somorjai, Langmuir **14**, 1458 (1998).
[6] S. C. Street, C. Xu, and D. W. Goodman, Annu. Rev. Phys. Chem. **48**, 43 (1997).
[7] Z. Tian, B. Ren, and D. Wu, J. Phys. Chem. B **106**, 9463 (2002).
[8] P. C. Anderson and K. L. Rowlen, Appl. Spectrosc. **56**, 124A (2002).
[9] H. Metiu and P. Das, Annu. Rev. Phys. Chem. **35**, 507 (1984).
[10] M. Moskovits, Rev. Mod. Phys. **57**, 783 (1985).
[11] K. Kneipp, H. Kneipp, I. Itzkan, R. R. Dasari, and M. S. Feld, Chem. Rev. (Washington, D.C.) **99**, 2957 (1999).
[12] H. Xu, E. J. Bjerneld, M. Kall, and L. Borjesson, Phys. Rev. Lett. **83**, 4357 (1999).
[13] S. Nie and S. R. Emory, Science **275**, 1102 (1997).
[14] K. Kneipp, Y. Wang, H. Kneipp, L. T. Perelman, I. Itzkan, R. R. Dasari, and M. S. Feld, Phys. Rev. Lett. **78**, 1667 (1997).
[15] A. M. Michaels, M. Nirmal, and L. E. Brus, J. Am. Chem. Soc. **121**, 9932 (1999).
[16] P. F. Liao, J. G. Bergman, D. S. Chemla, A. Wokaun, J. Melngailis, A. M. Hawryluk, and N. P. Economou, Chem. Phys. Lett. **82**, 355 (1981).
[17] M. D. Musick, C. D. Keating, L. A. Lyon *et al.*, Chem. Mater. **12**, 2869 (2000).
[18] T. Zhu, H. Z. Yu, J. Wang, Y. Q. Wang, S. M. Cai, and Z. F. Liu, Chem. Phys. Lett. **265**, 334 (1997).
[19] W. Kim, V. P. Safonov, V. M. Shalaev, and R. L. Armstrong, Phys. Rev. Lett. **82**, 4811 (1999).
[20] V. A. Markel, V. M. Shalaev, P. Zhang, W. Huynh, L. Tay, T. L. Haslett, and M. Moskovits, Phys. Rev. B **59**, 10903 (1999).
[21] J. C. Hulteen and R. P. Van Duyne, J. Vac. Sci. Technol. A **13**, 1553 (1995).
[22] C. L. Haynes and R. P. Van Duyne, J. Phys. Chem. B **105**, 5599 (2001).
[23] C. L. Haynes and R. P. Van Duyne, J. Phys. Chem. B **107**, 7426 (2003).
[24] H. A. Bullen and S. J. Garrett, Nano Lett. **2**, 739 (2002).
[25] T. R. Jensen, G. C. Schatz, and R. P. Van Duyne, J. Phys. Chem. B **103**, 2394 (1999).